*The Canadian Mineralogist*
Vol. 52, pp. 423-432 (2014)
DOI: 10.3749/canmin.52.3.423

# CAMERONITE, $Cu_{5-x}(Cu,Ag)_{3+x}Te_{10}$ ($x$ = 0.43), FROM THE GOOD HOPE MINE, VULCAN, COLORADO: CRYSTAL STRUCTURE AND REVISION OF THE CHEMICAL FORMULA

LUCA BINDI[§]

*Dipartimento di Scienze della Terra, Università degli Studi di Firenze, Via G. La Pira 4, I-50121 Firenze, Italy and CNR – Istituto di Geoscienze e Georisorse, Sezione di Firenze, Via G. La Pira 4, I-50121 Firenze, Italy*

WILLIAM W. PINCH

*19 Stonebridge Lane, Pittsford, New York 14534, U.S.A.*

## ABSTRACT

The crystal structure of the mineral cameronite, a rare copper-silver telluride, was solved using intensity data collected from a crystal of the holotype material from the Good Hope mine, Vulcan, Colorado (USA). The study revealed that the structure is monoclinic, space group $C2/c$, with cell parameters: $a$ 17.906(1), $b$ 17.927(1), $c$ 21.230(2) Å, β 98.081(8)°, and $V$ 6747.2(8) Å$^3$. The refinement of an anisotropic model led to an $R$ index of 0.0216 for 9688 independent reflections. Nineteen Te sites and 14 metal (M) sites occur in the crystal structure of cameronite. Six M sites host Cu with variable amounts of Ag, whereas the remaining eight M sites host Cu only. All of the atoms are in tetrahedral coordination and complex $MTe_4$, $M(Te_3M)$, $M(Te_2M_2)$, $TeM_4$, $Te(M_3Te)$, $Te(M_2Te_2)$, $Te(MTe_3)$, and $TeTe_4$ crystal-chemical environments are formed, as is typical of many intermetallic compounds. The short bond distances observed mainly among the Te atoms are discussed in relation to other copper and silver tellurides and pure metals. Electron microprobe analyses of the crystal used for the structural study led to the formula $Cu_{7.08}Ag_{1.06}Fe_{0.01}S_{0.01}Te_{9.84}$, on the basis of 18 atoms. On the basis of information gained from the structural and chemical characterization, the crystal-chemical formula was revised, yielding $Cu_{5-x}(Cu,Ag)_{3+x}Te_{10}$ ($Z$ 14) with $x$ = 0.43 instead of $Cu_7AgTe_{10}$ ($Z$ 16) as previously reported.

*Keywords*: cameronite, crystal structure, tellurides, Good Hope, Colorado

## INTRODUCTION

Cameronite was defined as a new mineral species with the chemical formula $Cu_7AgTe_{10}$ by Roberts *et al.* (1986) during a study of ores from the Good Hope mine, Vulcan, Colorado (USA). By means of X-ray photographic techniques (precession method), these authors studied four fragments of cameronite from a structural point of view and reported a tetragonal symmetry (with $P4_2/mmc$, $P4_2mc$, or $P\bar{4}2c$ as possible space groups) with $a$ 12.695(2), $c$ 42.186(6) Å, $V$ 6798.8(3.1) Å$^3$ and $Z$ = 16. Roberts *et al.* (1986) also noticed that the strongest X-ray reflections defined a subcell with $a' = a/3$ = 4.232 and $c' = c/7$ = 6.027 Å, and that the precession single-crystal films were dominated by $hkl$ reflections with $h,k$ = 3n and $l$ = 7n.

Interestingly, a mineral with the same physical, optical, chemical, and diffraction characteristics had already been described by Cameron & Threadgold (1961) in their paper describing the mineral species vulcanite. These authors also carried out single-crystal studies which suggested a hexagonal symmetry. Although Roberts *et al.* (1986) concluded that the unknown phase studied by Cameron & Threadgold (1961) and cameronite were the same phase, they failed to locate any symmetry element in support of the hexagonal symmetry and the reason for such a difference (tetragonal *versus* hexagonal) remained unresolved at that time.

In the course of a research project dealing with the description and structural characterization of natural copper and silver tellurides (Bindi & Cipriani 2004a,

§ Corresponding Author; e-mail address: luca.bindi@unifi.it

2004b, 2004c, Bindi 2008, 2009, Bindi *et al.* 2004, 2005, 2009, 2013), we have examined a fragment from the holotype material (sample R-934) obtained in 1974 by one of us (WWP) on exchange from the Smithsonian Institution, Washington, D.C. (USA). The sample consists of large rickardite grains associated with vulcanite, cameronite, native tellurium, and arsenopyrite.

To help resolve the concerns relating to the structure of cameronite and those related to the different symmetry reported for cameronite in the literature, we present new crystal structure data for the mineral from its type locality, together with new chemical data.

## Crystal-Structure Solution and Refinement

A small crystal fragment (65 × 85 × 115 μm) was selected for the single-crystal X-ray diffraction study. The intensity data collection (see Table 1 for details) was carried out by means of an Oxford Diffraction Xcalibur 3 single-crystal diffractometer (enhanced X-ray source, X-ray radiation MoKα, λ = 0.71073 Å) fitted with a Sapphire 2 CCD detector. A total of 1589 frames of data were collected at room temperature as eight sets of omega runs with an exposure time of 45 s per frame and a frame width of 1.00°. This afforded an overall data collection of 78245 reflections (9688 unique). The refined monoclinic unit-cell parameters are *a* 17.906(1), *b* 17.927(1), *c* 21.230(2) Å, β 98.081(8)°, and *V* 6747.2(8) Å$^3$, which are related, neglecting the monoclinic distortion, to those found by Roberts *et al.* (1986) [*a* 12.695(2), *c* 42.186(6) Å, *V* 6798.8(3.1) Å$^3$] by the following transformation matrix [½,½,0/½,–½,0/0,0,$\bar{2}$]. The presence of a tetragonal substructure with *a*' ≈ 4.2 and *c*' ≈ 6.03 Å was confirmed, and found to be due to the typical disordered 'rickardite-type' basic structure (Forman & Peacock 1949, Schutte & de Boer 1993).

Data frames were processed using the *CrysAlis* software package (Oxford Diffraction 2006) running on the Xcalibur 3 control PC. The program ABSPACK (Oxford Diffraction 2006) was used for the absorption correction. The merging *R* for the data set decreased from 14.25% before the absorption correction to 3.66% after the correction. The observed reflection conditions (*hkl*: *h*+*k* = 2*n*; *h*0*l*: *h*,*l* = 2*n*; 0*kl*: *k* = 2*n*; *hk*0: *h*+*k* = 2*n*; 0*k*0: *k* = 2*n*; *h*00: *h* = 2*n*; 00*l*: *l* = 2*n*), together with the statistical tests on the distribution of |E| values that strongly indicated the presence of an inversion center ($|E^2 - 1| = 0.976$), suggested space group *C*2/*c*. The structure solution was then initiated in this space group. The positions of most of the atoms (all the M positions and most of the Te atoms) were determined by means of direct methods (Sheldrick 2008). A least-squares refinement on $F^2$ using these heavy-atom positions and isotropic temperature factors produced an *R* factor of 0.165. Three-dimensional difference Fourier synthesis yielded the position of the remaining Te atoms. The SHELXL program (Sheldrick 2008) was used for the refinement of the structure. The occupancy of all the sites was left free to vary (Ag *versus* vacancy for the M sites; Te *versus* vacancy). The occupancy of eight M sites (M7–M14; Table 2) was found to be consistent with complete occupation by Cu and then fixed to the resulting value. Neutral scattering curves for Ag, Cu, and Te were taken from the *International Tables for X-ray Crystallography* (Ibers & Hamilton 1974). In the final stage, with anisotropic atomic displacement parameters for all atoms and no constraints, the residual value settled at *R* = 0.0210 for 3839 observed reflections [$F_o > 4\sigma(F_o)$ level] and 292 parameters, and at *R* = 0.0216 for all 9688 independent reflections. Inspection

TABLE 1. DATA AND EXPERIMENTAL DETAILS FOR THE SELECTED CAMERONITE CRYSTAL

| | |
|---|---|
| **Crystal data** | |
| Formula | $Cu_{5-x}(Cu,Ag)_{3+x}Te_{10}$ (with *x* = 0.43) |
| Crystal size (mm) | 0.065 × 0.085 × 0.115 |
| Form | block |
| Color | black |
| Crystal system | monoclinic |
| Space group | *C*2/*c* (#15) |
| *a* (Å) | 17.906(1) |
| *b* (Å) | 17.927(1) |
| *c* (Å) | 21.230(2) |
| β (°) | 98.081(8) |
| *V* (Å$^3$) | 6747.2(8) |
| *Z* | 14 |
| **Data collection** | |
| Instrument | Oxford Diffraction Xcalibur 3 |
| Radiation type | Mo*K*α (λ = 0.71073) |
| Temperature (K) | 293(3) |
| Detector to sample distance (cm) | 6 |
| Number of frames | 1589 |
| Measuring time (s) | 45 |
| Maximum covered 2θ (°) | 59.99 |
| Absorption correction | multi-scan (*ABSPACK*; Oxford Diffraction 2006) |
| Collected reflections | 78245 |
| Unique reflections | 9688 |
| Reflections with $F_o > 4\sigma(F_o)$ | 3839 |
| $R_{int}$ | 0.0366 |
| $R_\sigma$ | 0.0582 |
| Range of *h*, *k*, *l* | $-25 \le h \le 25$, $-25 \le k \le 25$, $-29 \le l \le 29$ |
| **Refinement** | |
| Refinement | Full-matrix least squares on $F^2$ |
| Final $R_1$ [$F_o > 4\sigma(F_o)$] | 0.0210 |
| Final $R_1$ (all data) | 0.0216 |
| Number refined parameters | 292 |
| $\Delta\rho_{max}$ (e Å$^{-3}$) | 1.47 |
| $\Delta\rho_{min}$ (e Å$^{-3}$) | –2.01 |

TABLE 2. ATOMS, SITE OCCUPANCY FACTORS (s.o.f.), ATOMIC COORDINATES, AND EQUIVALENT ISOTROPIC DISPLACEMENT PARAMETERS (Å$^2$) FOR THE SELECTED CAMERONITE CRYSTAL

| Atom | s.o.f. | *x/a* | *y/b* | *z/c* | $U_{eq}$ |
|---|---|---|---|---|---|
| M1 | $Cu_{0.78(1)}Ag_{0.22}$ | 0.115992(9) | 0.045060(7) | –0.036220(7) | 0.01961(5) |
| M2 | $Cu_{0.69(1)}Ag_{0.31}$ | 0.209464(9) | –0.042355(6) | 0.030806(7) | 0.01957(5) |
| M3 | $Cu_{0.92(1)}Ag_{0.08}$ | 0.733704(8) | 0.291402(6) | 0.175078(7) | 0.01447(5) |
| M4 | $Cu_{0.57(1)}Ag_{0.43}$ | 0.54814(1) | –0.041555(7) | 0.028293(9) | 0.02767(5) |
| M5 | $Cu_{0.70(1)}Ag_{0.30}$ | –0.093670(9) | 0.879470(9) | 0.675700(8) | 0.02702(6) |
| M6 | $Cu_{0.59(1)}Ag_{0.41}$ | –0.070723(8) | 0.043392(7) | 0.822239(6) | 0.02390(5) |
| M7 | $Cu_{1.00}$ | 0.38291(1) | 0.788241(9) | 0.032437(9) | 0.02171(4) |
| M8 | $Cu_{1.00}$ | 0.573341(9) | 0.126046(8) | 0.176352(8) | 0.02044(5) |
| M9 | $Cu_{1.00}$ | 0.76177(1) | 0.457468(9) | 0.323851(9) | 0.02501(5) |
| M10 | $Cu_{1.00}$ | 0.40567(1) | –0.042242(9) | 0.176939(9) | 0.02447(5) |
| M11 | $Cu_{1.00}$ | 0.93115(1) | 0.291467(8) | 0.323874(8) | 0.02066(5) |
| M12 | $Cu_{1.00}$ | 0.59096(1) | 0.293941(8) | 0.320657(7) | 0.02025(5) |
| M13 | $Cu_{1.00}$ | 0.26180(1) | 0.374311(9) | 0.822078(8) | 0.02389(5) |
| M14 | $Cu_{1.00}$ | 0.71466(1) | 0.124980(9) | 0.035825(9) | 0.02241(5) |
| Te1 | $Te_{1.00}$ | 0.5 | 0.041272(5) | 0.25 | 0.01766(3) |
| Te2 | $Te_{1.00}$ | 0 | 0.210338(6) | 0.25 | 0.02099(3) |
| Te3 | $Te_{1.00}$ | 0 | 0.123149(6) | 0.75 | 0.02071(3) |
| Te4 | $Te_{1.00}$ | 0.835113(4) | 0.376439(4) | 0.251411(3) | 0.02200(3) |
| Te5 | $Te_{1.00}$ | 0.358290(4) | 0.288967(4) | –0.108482(3) | 0.02135(3) |
| Te6 | $Te_{1.00}$ | 0.666249(5) | 0.206467(4) | 0.251036(4) | 0.02069(3) |
| Te7 | $Te_{1.00}$ | 0.311121(4) | 0.041591(3) | 0.109886(4) | 0.02157(3) |
| Te8 | $Te_{1.00}$ | 0.478428(5) | –0.122799(4) | 0.110142(4) | 0.02300(3) |
| Te9 | $Te_{1.00}$ | 0.194542(6) | 0.123686(5) | –0.108793(4) | 0.02388(3) |
| Te10 | $Te_{1.00}$ | 0.641929(6) | 0.039075(5) | 0.111922(6) | 0.02365(3) |
| Te11 | $Te_{1.00}$ | 0.476675(6) | 0.204339(6) | 0.110747(5) | 0.02075(3) |
| Te12 | $Te_{1.00}$ | 0.831844(6) | –0.041590(5) | 0.747907(5) | 0.02551(3) |
| Te13 | $Te_{1.00}$ | 0.025378(7) | –0.041174(5) | –0.107167(6) | 0.02215(4) |
| Te14 | $Te_{1.00}$ | 0.646378(6) | 0.376196(5) | 0.106946(5) | 0.02412(3) |
| Te15 | $Te_{1.00}$ | 0.809574(5) | 0.208891(4) | 0.111224(4) | 0.01983(3) |
| Te16 | $Te_{1.00}$ | 0.452296(7) | 0.376501(5) | –0.036558(5) | 0.02051(3) |
| Te17 | $Te_{1.00}$ | 0.546182(7) | 0.293549(5) | 0.036913(6) | 0.02190(4) |
| Te18 | $Te_{1.00}$ | 0.378792(8) | 0.126708(6) | 0.029071(7) | 0.02185(3) |
| Te19 | $Te_{1.00}$ | 0.284180(6) | 0.210017(4) | –0.032196(5) | 0.02119(3) |

of the difference Fourier map revealed that maximum positive and negative peaks were 1.47 and 2.01 e$^-$/Å$^3$, respectively. Experimental details and *R* indices are given in Table 1. Fractional atomic coordinates and isotropic displacement parameters are reported in Table 2, whereas the anisotropic displacement parameters are given in Table 3. A list of the observed and calculated structure factors is available from the Depository of Unpublished Data, MAC website [document Cameronite CM52_423].

## Chemical Composition

The chemical composition was determined using wavelength dispersive analysis (WDS) conducted with a JEOL JXA-8200 electron microprobe from the same crystal used for the structural study. Concentrations of major and minor elements were determined at an accelerating voltage of 20 kV and a beam current of 40 nA, with 10 s as the counting time. For the WDS analyses the following lines were used: S*K*α, Fe*K*α, Cu*K*α, Zn*K*α, As*L*α, Se*L*α, Ag*L*α, Sb*L*β, Te*L*α, Pb*M*α, and Bi*M*β. The standards employed were: native elements for Cu and Ag, galena for Pb, pyrite for Fe and S, synthetic $Sb_2Te_3$ for Sb and Te, synthetic $As_2S_3$ for As, synthetic $Bi_2S_3$ for Bi, synthetic ZnS for Zn, and synthetic $PtSe_2$ for Se. The crystal fragment was found to be homogeneous within analytical uncertainty. The average chemical compositions (six analyses from different spots), together with ranges of wt.% of elements, are reported in Table 4. On the basis of 18 atoms, the chemical formula for cameronite can be written as $Cu_{7.08}Ag_{1.06}Fe_{0.01}S_{0.01}Te_{9.84}$ or, according to the revised chemical formula obtained on the basis of the structural results (see below), $Cu_{5-x}(Cu,Ag)_{3+x}Te_{10}$ with $x = 0.43$.

TABLE 3. ANISOTROPIC DISPLACEMENT PARAMETERS OF THE ATOMS FOR THE SELECTED CAMERONITE CRYSTAL

| | $U_{11}$ | $U_{22}$ | $U_{33}$ | $U_{12}$ | $U_{13}$ | $U_{23}$ |
|---|---|---|---|---|---|---|
| M1 | 0.01992(8) | 0.01966(7) | 0.01927(8) | 0.00002(4) | 0.00285(5) | –0.00002(4) |
| M2 | 0.01992(8) | 0.01955(7) | 0.01927(7) | 0.00001(3) | 0.00281(5) | 0.00002(3) |
| M3 | 0.01476(8) | 0.01450(7) | 0.01420(7) | –0.00003(3) | 0.00217(4) | 0.00003(3) |
| M4 | 0.02794(9) | 0.02769(8) | 0.02735(8) | 0.00001(4) | 0.00380(5) | –0.00002(4) |
| M5 | 0.02732(9) | 0.02698(8) | 0.02676(8) | –0.00001(4) | 0.00383(6) | –0.00003(4) |
| M6 | 0.02407(9) | 0.02397(8) | 0.02364(8) | 0.00005(4) | 0.00329(5) | –0.00003(4) |
| M7 | 0.02196(9) | 0.02168(8) | 0.02149(8) | 0.00001(5) | 0.00310(6) | 0.00013(5) |
| M8 | 0.02082(9) | 0.02035(8) | 0.02023(8) | –0.00002(4) | 0.00320(6) | 0.00000(4) |
| M9 | 0.0253(1) | 0.02501(9) | 0.02472(9) | –0.00011(5) | 0.00364(7) | 0.00009(5) |
| M10 | 0.0247(1) | 0.02458(9) | 0.02422(9) | –0.00005(5) | 0.00364(7) | –0.00002(5) |
| M11 | 0.02105(9) | 0.02067(8) | 0.02028(8) | –0.00002(4) | 0.00300(6) | –0.00002(4) |
| M12 | 0.02046(9) | 0.02019(8) | 0.02011(8) | –0.00004(4) | 0.00294(6) | –0.00002(4) |
| M13 | 0.0241(1) | 0.02392(9) | 0.02366(9) | –0.00008(5) | 0.00336(7) | 0.00004(5) |
| M14 | 0.02272(9) | 0.02240(8) | 0.02210(8) | –0.00002(5) | 0.00312(7) | 0.00001(5) |
| Te1 | 0.02055(6) | 0.02102(5) | 0.02038(6) | 0 | 0.00291(4) | 0 |
| Te2 | 0.02136(6) | 0.02095(6) | 0.02067(6) | 0 | 0.00301(4) | 0 |
| Te3 | 0.02102(6) | 0.02069(5) | 0.02043(6) | 0 | 0.00294(4) | 0 |
| Te4 | 0.02266(5) | 0.02238(4) | 0.02104(4) | 0.00002(2) | 0.00217(3) | 0.00003(2) |
| Te5 | 0.02255(4) | 0.02036(4) | 0.02208(4) | 0.00003(2) | 0.00251(3) | –0.00002(2) |
| Te6 | 0.02100(5) | 0.02072(5) | 0.02036(5) | 0.00005(2) | 0.00237(3) | –0.00002(2) |
| Te7 | 0.02091(5) | 0.02259(4) | 0.02122(4) | 0.00001(2) | 0.00208(3) | 0.00001(2) |
| Te8 | 0.02329(5) | 0.02203(4) | 0.02268(4) | –0.00002(2) | 0.00220(3) | –0.00002(2) |
| Te9 | 0.02213(5) | 0.02187(5) | 0.02064(5) | 0.00001(2) | 0.00218(4) | 0.00000(2) |
| Te10 | 0.02291(6) | 0.02267(5) | 0.02236(6) | –0.00003(3) | 0.00215(4) | –0.00003(3) |
| Te11 | 0.02104(6) | 0.02074(5) | 0.02045(6) | –0.00006(3) | 0.00227(4) | –0.00001(3) |
| Te12 | 0.02177(6) | 0.02250(5) | 0.02224(5) | –0.00001(3) | 0.00256(4) | 0.00004(3) |
| Te13 | 0.02240(7) | 0.02215(6) | 0.02190(6) | 0.00004(3) | 0.00256(5) | –0.00004(3) |
| Te14 | 0.02456(5) | 0.02406(5) | 0.02374(5) | 0.00000(2) | 0.00243(4) | –0.00004(2) |
| Te15 | 0.02010(5) | 0.01986(5) | 0.01954(5) | 0.00004(2) | 0.00283(3) | 0.00001(2) |
| Te16 | 0.02076(6) | 0.02152(5) | 0.02028(5) | –0.00002(3) | 0.00210(4) | 0.00002(3) |
| Te17 | 0.02223(6) | 0.02187(5) | 0.02160(6) | 0.00003(3) | 0.00227(4) | –0.00001(3) |
| Te18 | 0.02209(6) | 0.02215(6) | 0.02203(6) | –0.00004(3) | 0.00234(4) | 0.00001(3) |
| Te19 | 0.02143(5) | 0.02122(5) | 0.02094(5) | –0.00004(2) | 0.00202(3) | 0.00001(2) |

TABLE 4. ELECTRON MICROPROBE DATA AND ATOMIC RATIOS WITH THEIR STANDARD DEVIATIONS (σ) FOR THE SELECTED CAMERONITE CRYSTAL

| | wt.% | Range | atomic ratios | σ |
|---|---|---|---|---|
| Ag | 6.25 | 6.10–6.66 | 1.06 | 0.05 |
| Cu | 24.49 | 24.11–25.09 | 7.08 | 0.15 |
| Bi | 0.01 | 0.00–0.04 | - | - |
| Pb | 0.01 | 0.00–0.03 | - | - |
| Zn | 0.01 | 0.00–0.04 | - | - |
| Fe | 0.02 | 0.00–0.06 | 0.01 | 0.01 |
| Sb | 0.01 | 0.00–0.02 | - | - |
| As | 0.01 | 0.00–0.03 | - | - |
| S | 0.01 | 0.00–0.02 | 0.01 | 0.01 |
| Se | 0.02 | 0.00–0.05 | - | - |
| Te | 68.35 | 67.50–69.11 | 9.84 | 0.14 |
| Total | 99.19 | 98.90–100.55 | | |

The means and ranges of electron microprobe data are in wt.% of elements. Atomic ratios are on the basis of 18 atoms.

## Description of the Structure and Discussion

The crystal structure of cameronite (Figs. 1 and 2) represents a new structure type in the Cu–Te system (see Pashinkin & Fedorov 2003 for a review). It can be considered an intermetallic compound and, therefore, the classic polyhedral description is hardly applicable. There are 19 independent Te sites and 14 metal (M) sites in the crystal structure with Z = 14. The calculated density for cameronite is therefore 6.303 g/cm$^3$ and not 7.144 g/cm$^3$ as previously hypothesized on the basis of Z = 16 (Roberts *et al.* 1986).

In the structure, six M sites (M1–M6; Table 2) host Cu with variable amounts of Ag (from 0.08 to 0.41 *apfu*), whereas the remaining eight M sites (M7–M14; Table 2) host Cu only. All the atoms are in tetrahedral coordination and complex $MTe_4$, $M(Te_3M)$, $M(Te_2M_2)$, $TeM_4$, $Te(M_3Te)$, $Te(M_2Te_2)$, $Te(MTe_3)$, $TeTe_4$ crystal-chemical environments are formed (Table 5). The presence of Ag substituting for Cu at some of the M sites

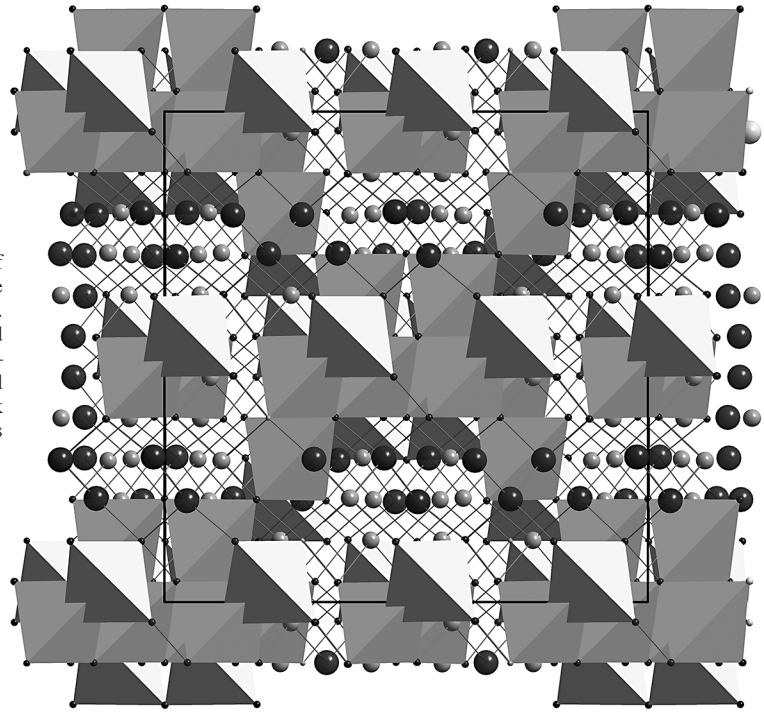

FIG. 1. The crystal structure of cameronite down [001]. The horizontal direction is the *a* axis. The M1–M6 atoms are depicted as tetrahedra whereas the M7–M14 atoms are shown as small light grey spheres; Te: large dark grey spheres. The unit cell is outlined.

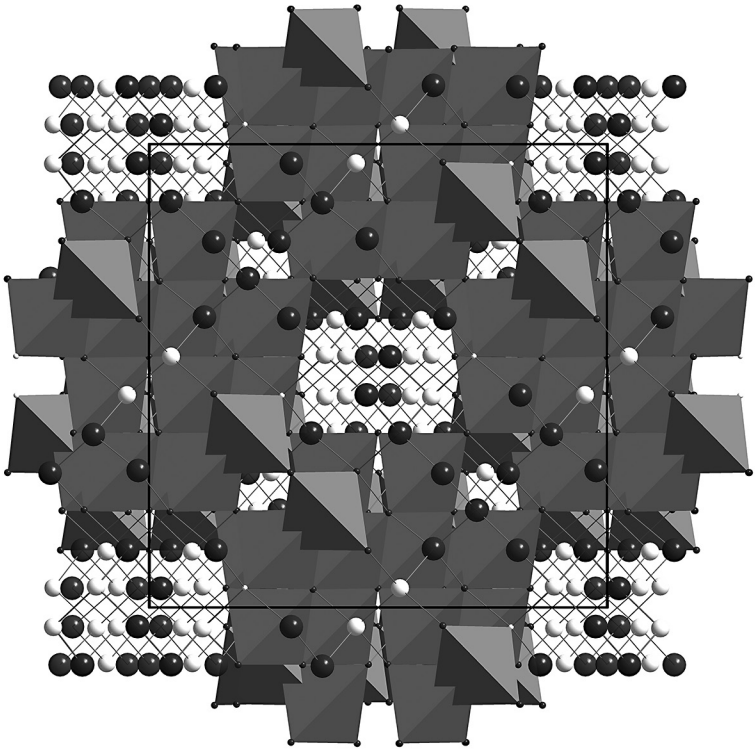

FIG. 2. The crystal structure of cameronite down [001]. The horizontal direction is the *a* axis. The M7–M14 atoms are depicted as tetrahedra whereas the M1–M6 atoms are shown as small white spheres; Te: large dark grey spheres. The unit-cell is outlined.

TABLE 5. BOND DISTANCES (IN Å) IN THE STRUCTURE OF CAMERONITE

| | | | | | | | |
|---|---|---|---|---|---|---|---|
| **M1** | | **M9** | | **Te4** | | **Te12** | |
| Te16 | 2.5280(3) | Te9 | 2.4687(3) | M9 | 2.6015(2) | M9 | 2.5859(3) |
| Te13 | 2.5698(3) | Te10 | 2.5124(3) | M10 | 2.6044(2) | M5 | 2.5897(3) |
| M2 | 2.5714(3) | Te12 | 2.5859(3) | M11 | 2.6268(3) | M13 | 2.6231(2) |
| Te9 | 2.6359(2) | Te4 | 2.6015(2) | M3 | 2.7240(2) | M6 | 2.6610(2) |
| mean | 2.5763 | mean | 2.5421 | mean | 2.6392 | mean | 2.6149 |
| **M2** | | **M10** | | **Te5** | | **Te13** | |
| Te14 | 2.5562(2) | Te8 | 2.5126(3) | M11 | 2.5239(2) | M5 | 2.4771(3) |
| M14 | 2.5654(3) | Te7 | 2.5444(3) | M13 | 2.6044(3) | M1 | 2.5698(3) |
| M1 | 2.5714(3) | Te1 | 2.6007(3) | Te16 | 2.6277(2) | Te16 | 2.5863(2) |
| Te7 | 2.7454(3) | Te4 | 2.6044(2) | Te19 | 2.6441(2) | M6 | 2.6039(3) |
| mean | 2.6096 | mean | 2.5655 | mean | 2.6000 | mean | 2.5593 |
| **M3** | | **M11** | | **Te6** | | **Te14** | |
| Te14 | 2.4924(2) | Te8 | 2.5117(2) | M13 | 2.5639(3) | M3 | 2.4924(2) |
| Te15 | 2.5277(2) | Te5 | 2.5239(2) | M8 | 2.5726(3) | M2 | 2.5562(2) |
| Te6 | 2.6316(2) | Te2 | 2.5766(2) | M3 | 2.6316(2) | M6 | 2.5973(2) |
| Te4 | 2.7240(2) | Te4 | 2.6268(3) | M12 | 2.6498(2) | Te17 | 2.6220(2) |
| mean | 2.5939 | mean | 2.5598 | mean | 2.6045 | mean | 2.5670 |
| **M4** | | **M12** | | **Te7** | | **Te15** | |
| Te18 | 2.4440(3) | Te3 | 2.5348(3) | M10 | 2.5444(3) | M3 | 2.5277(2) |
| M4 | 2.4603(4) | Te11 | 2.5814(2) | M13 | 2.5680(2) | M5 | 2.5919(2) |
| Te10 | 2.6876(3) | Te6 | 2.6498(2) | Te18 | 2.7064(2) | M14 | 2.6360(3) |
| Te8 | 2.7035(3) | Te9 | 2.6614(3) | M2 | 2.7454(3) | M7 | 2.6764(3) |
| mean | 2.5739 | mean | 2.6069 | mean | 2.6411 | mean | 2.6080 |
| **M5** | | **M13** | | **Te8** | | **Te16** | |
| Te13 | 2.4771(3) | Te6 | 2.5639(3) | M11 | 2.5117(3) | M1 | 2.5280(3) |
| Te12 | 2.5897(2) | Te7 | 2.5680(2) | M10 | 2.5126(3) | Te13 | 2.5863(2) |
| Te15 | 2.5919(2) | Te5 | 2.6044(3) | M4 | 2.7035(3) | Te17 | 2.5949(2) |
| Te2 | 2.6739(3) | Te12 | 2.6231(3) | M7 | 2.7197(3) | Te5 | 2.6277(2) |
| mean | 2.5832 | mean | 2.5899 | mean | 2.6119 | mean | 2.5842 |
| **M6** | | **M14** | | **Te9** | | **Te17** | |
| Te3 | 2.5585(2) | M2 | 2.5654(3) | M9 | 2.4687(3) | M7 | 2.5407(3) |
| Te14 | 2.5973(2) | M7 | 2.6194(3) | Te19 | 2.6234(2) | Te16 | 2.5949(2) |
| Te13 | 2.6039(3) | Te15 | 2.6360(3) | M1 | 2.6359(2) | Te14 | 2.6220(2) |
| Te12 | 2.6610(2) | Te10 | 2.6962(3) | M12 | 2.6614(3) | Te11 | 2.6669(2) |
| mean | 2.6052 | mean | 2.6293 | mean | 2.5974 | mean | 2.6061 |
| **M7** | | **Te1** | | **Te10** | | **Te18** | |
| Te17 | 2.5407(3) | M10 (×2) | 2.6007(3) | M8 | 2.5065(3) | M4 | 2.4440(3) |
| M14 | 2.6194(3) | M8 (×2) | 2.6564(2) | M9 | 2.5124(3) | Te19 | 2.4845(2) |
| Te15 | 2.6764(3) | mean | 2.6286 | M4 | 2.6876(3) | Te11 | 2.6760(3) |
| Te8 | 2.7197(3) | | | M14 | 2.6962(3) | Te7 | 2.7064(2) |
| mean | 2.6391 | **Te2** | | mean | 2.6007 | mean | 2.5777 |
| | | M11 (×2) | 2.5766(2) | | | | |
| **M8** | | M5 (×2) | 2.6739(3) | **Te11** | | **Te19** | |
| Te11 | 2.4956(3) | mean | 2.6253 | M8 | 2.4956(3) | Te19 | 2.4275(2) |
| Te10 | 2.5065(3) | | | M12 | 2.5814(2) | Te18 | 2.4845(2) |
| Te6 | 2.5726(3) | **Te3** | | Te17 | 2.6669(2) | Te9 | 2.6234(2) |
| Te1 | 2.6564(2) | M12 (×2) | 2.5348(2) | Te18 | 2.6760(3) | Te5 | 2.6441(2) |
| mean | 2.5578 | M6 (×2) | 2.5585(2) | mean | 2.6050 | mean | 2.5449 |
| | | mean | 2.5467 | | | | |

(M1–M6) does not affect the bond distances (mean bond distances in the range 2.54–2.64 Å). Similarly, the Te-tetrahedra show mean bond distances in the range 2.54–2.64 Å, independent of the crystal-chemical environment adopted. Figures 3 and 4 show typical examples of "interpenetrated tetrahedra" that can be seen in the cameronite structure. Such a peculiar structural situation promotes the occurrence of very short bond distances between atoms. The shortest (Cu,Ag)–Te distance in cameronite of 2.4440(3) Å (*i.e.*, M4–Te18) is indeed much shorter than the 2.604(1) Å and 2.63(1) Å observed in vulcanite (CuTe, Pertlik 2001) and in the average structure of rickardite ($Cu_{3-x}Te_2$, Schutte & de Boer 1993), respectively. A similar behavior is

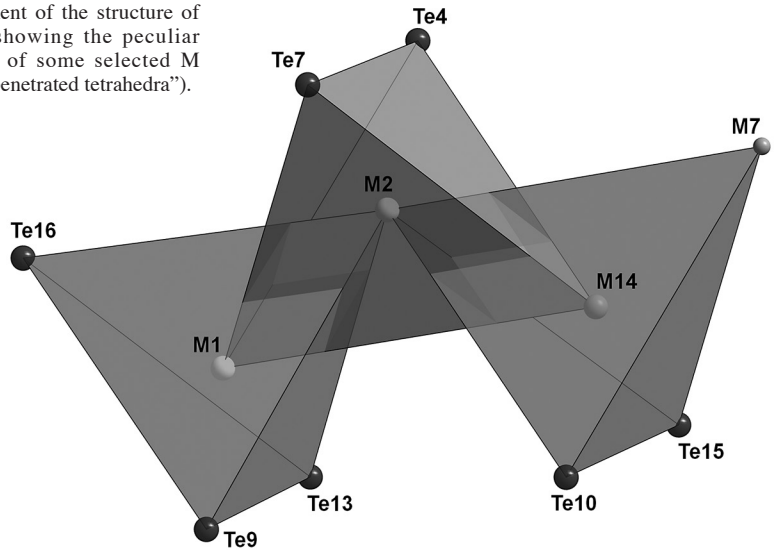


FIG. 3. A fragment of the structure of cameronite showing the peculiar coordination of some selected M atoms ("interpenetrated tetrahedra").

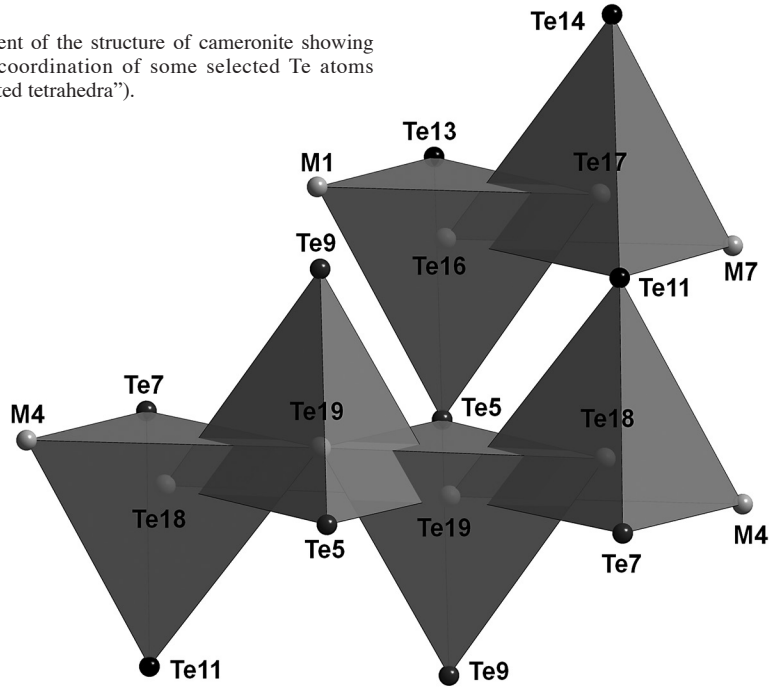


FIG. 4. A fragment of the structure of cameronite showing the peculiar coordination of some selected Te atoms ("interpenetrated tetrahedra").

observable for the Cu–Cu and Te–Te contacts: the shortest Cu–Cu distance (*i.e.*, M4–M4) of 2.4603(4) Å is shorter than that observed in metallic copper (2.546 Å; Suh *et al.* 1988) and the shortest Te–Te distance (*i.e.*, Te19–Te19) of 2.4275(2) Å is shorter than that observed in native tellurium (Te–Te = 2.835 Å, Cherin & Unger 1967). The same features have been observed in the structure of weissite (Bindi *et al.* 2013), which shows even shorter Cu–Te [2.308(2) Å] and Cu–Cu [2.282(3) Å] distances and similar Te–Te [2.496(1) Å] contacts.

Weissite and cameronite can be considered as complex superstructures of the basic tetragonal *P*4/*nmm* substructure with $a' \approx 4.2$ and $c' \approx 6.03$ Å (the disordered 'rickardite-type' basic structure; Forman & Peacock 1949, Schutte & de Boer 1993) where the arrangement of the Cu (and Ag) ions depends on the composition of the phase and thermal history. The formation of such superstructures, as others have observed in the Cu–Te system (Blachnik *et al.* 1983, Pashinkin & Fedorov 2003), is generally ascribed to the mobility of the copper ions in different valence states, $Cu^{+}$ or $Cu^{2+}$, in a rigid Te framework. The presence of Ag in cameronite seems fundamental to stabilize the new structure type never before recognized in the deeply studied Cu–Te system. However, Ag does not order at a specific site in the crystal structure of cameronite, as would be expected by its unitary stoichiometric content in the chemical formula when normalized on the basis of 18 atoms. This implies that the structure determined here could still be an average structure (although neither commensurate nor incommensurate satellites have been observed) and the real structure might be an even larger superstructure or, more likely, a complex incommensurately modulated structure like that observed in synthetic rickardite (Schutte & de Boer 1993) with a displacive modulation of the atoms associated with a $Cu^{+}/Cu^{2+}$ valence fluctuation. Such a phenomenon has also been observed in calaverite, $AuTe_2$, with a fluctuation between $Au^{+}$ and $Au^{3+}$ in the structure (Bindi *et al.* 2009).

Table 6 shows the X-ray powder pattern calculated using the structural data obtained in this study. It appears very similar to that reported by Roberts *et al.* (1986) for cameronite. The presence of two minor peaks (at 2.531 and 2.344 Å) reported in the original study (Roberts *et al.* 1986) and not present in the calculated pattern is noted. Possible reasons could be linked to the fact that cameronite exhibits complex intergrowths with rickardite and vulcanite.

## Acknowledgments

The X-ray intensity data were collected at CRIST, Centro di Cristallografia Strutturale, University of Florence, Italy. This work was funded by "Progetto d'Ateneo 2012" issued to LB. The paper benefited by the official reviews made by Cristian Biagioni and František Laufek.

TABLE 6. X-RAY POWDER DIFFRACTION DATA FOR CAMERONITE

| | 1 | | 2 | |
|---|---|---|---|---|
| *hkl* | $d_{calc}$ (Å) | $I_{calc}$ | $d_{obs}$ (Å) | $I_{rel}$ |
| –334 | 3.4544 | 100 | 3.456 | 100 |
| 333 | | | | |
| –335 | 3.1325 | 3 | - | - |
| 334 | | | | |
| 061 | 2.9581 | 5 | 2.958 | 20 |
| 008 | 2.6274 | 2 | 2.635 | 10 |
| - | - | - | 2.531 | 10 |
| - | - | - | 2.344 | 5 |
| 067 | 2.1180 | 25 | 2.118 | 100 |
| –608 | 2.1167 | 25 | | |
| 606 | | | | |
| –661 | 2.1115 | 26 | 1.815 | 30 |
| –33$\underline{11}$ | 1.8089 | 15 | | |
| 33$\underline{10}$ | | | | |
| –394 | 1.8024 | 15 | | |
| 393 | | | 1.804 | 60 |
| –935 | 1.8008 | 15 | | |
| 932 | | | | |
| –395 | 1.7516 | 2 | 1.755 | 3 |
| 394 | | | | |
| –936 | 1.7502 | 2 | | |
| 933 | | | | |

| | | | | |
|---|---|---|---|---|
| –669 | 1.6459 | 2 | 1.650 | 5 |
| 667 | | | | |
| 0014 | 1.5014 | 4 | 1.507 | 10 |
| 0120 | 1.4939 | 4 | 1.496 | 20 |
| –1202 | 1.4922 | 5 | | |
| –9312 | 1.3734 | 6 | 1.377 | 40 |
| 939 | | | | |
| –995 | 1.3705 | 8 | | |
| 992 | | | | |
| –6615 | 1.2236 | 7 | 1.227 | 20 |
| 6613 | | | | |
| –6128 | 1.2205 | 8 | | |
| 6126 | | | | |
| –1269 | 1.2198 | 8 | 1.222 | 40 |
| –1265 | | | | |
| –3318 | 1.1553 | 3 | 1.158 | 5 |
| 3317 | | | | |
| –9912 | 1.1515 | 3 | 1.151 | 30 |
| 999 | | | | |
| –3154 | 1.1502 | 3 | | |
| 3153 | | | | |
| –1536 | 1.1490 | 3 | | |
| 1531 | | | | |
| 01214 | 1.0590 | 2 | 1.062 | 10 |
| –12122 | 1.0557 | 2 | 1.058 | 5 |
| –3918 | 1.0136 | 2 | 1.017 | 10 |
| 3917 | | | | |
| –9319 | 1.0134 | 2 | 1.014 | 5 |
| 9316 | | | | |
| –31511 | 1.0113 | 2 | 1.012 | 20 |
| 31510 | | | | |
| –15313 | 1.0105 | 3 | | |
| 1538 | | | | |
| –9155 | 1.0099 | 2 | | |
| 9152 | | | | |
| –1596 | 1.0094 | 2 | | |
| 1591 | | | | |
| 0621 | 0.9491 | 1 | 0.9521 | 10 |
| 0187 | 0.9453 | 1 | 0.9465 | 30 |
| –6181 | 0.9447 | 1 | | |
| –1863 | 0.9438 | 1 | | |
| –9919 | 0.9137 | 2 | 0.9164 | 10 |
| 9916 | | | 0.9140 | 30 |

Notes: 1 = Calculated powder pattern and indexing for cameronite on the basis of *a* = 17.906(1), *b* = 17.927(1), *c* = 21.230(2) Å, β = 98.081(8)° and with the atom coordinates reported in Table 2. Intensities were calculated using XPOW software, version 2.0 (Downs *et al.* 1993). 2 = observed powder pattern originally reported by Roberts *et al.* (1986).

## References


Bindi, L. (2008) Commensurate-incommensurate phase transition in muthmannite, $AuAgTe_2$: First evidence of a modulated structure at low-temperature. *Philosophical Magazine Letters* **88**, 533–541.

Bindi, L. (2009) Thermal expansion behavior of empressite, AgTe: A structural study by means of in situ high-temperature single-crystal X-ray diffraction. *Journal of Alloys and Compounds* **473**, 262–264.

Bindi, L. & Cipriani, C. (2004a) Ordered distribution of Au and Ag in the crystal structure of muthmannite, $AuAgTe_2$, a rare telluride from Sacarîmb, western Romania. *American Mineralogist* **89**, 1505–1509.

Bindi, L. & Cipriani, C. (2004b) Structural and physical properties of fischesserite, a rare gold-silver selenide from the De Lamar Mine, Owyhee County, Idaho, USA. *Canadian Mineralogist* **42**, 1733–1737.

Bindi, L. & Cipriani, C. (2004c) Mazzettiite, $Ag_3HgPbSbTe_5$, a new mineral species for Findley Gulch, Saguache County, Colorado. *Canadian Mineralogist* **42**, 1739–1743.

Bindi, L., Spry, P.G., & Cipriani, C. (2004) Empressite, AgTe, from the Empress-Josephine Mine, Colorado, USA: composition, physical properties and determination of the crystal structure. *American Mineralogist* **89**, 1043–1047.

Bindi, L., Rossell Abrodos, M., Van Tendeloo, G., Spry, P.G., & Cipriani, C. (2005) Inferred phase relations in part of the system Au–Ag–Te: an integrated analytical study of gold ore from the Golden Mile, Kalgoorlie, Australia. *Mineralogy and Petrology* **83**, 283–293.

Bindi, L., Arakcheeva, A., & Chapuis, G. (2009) The role of silver on the stabilization of the incommensurately modulated structure in calaverite, $AuTe_2$. *American Mineralogist* **94**, 728–736.

Bindi, L., Carbone, C., Belmonte, D., Cabella, R., & Bracco, R. (2013) Weissite from Gambatesa mine, Val Graveglia, Liguria, Italy: occurrence, composition and determination of the crystal structure. *Mineralogical Magazine* **77**, 475–483.

Blachnik, R., Lasocka, M., & Walbrecht, U. (1983) The system copper-tellurium. *Journal of Solid State Chemistry* **48**, 431–438.

Cameron, E.N. & Threadgold, I.M. (1961) Vulcanite, a new copper telluride from Colorado, with notes on certain associated minerals. *American Mineralogist* **46**, 258–268.

Cherin, P. & Unger, P. (1967) Two-dimensional refinement of the crystal structure of tellurium. *Acta Crystallographica* **23**, 670–671.

Downs, R.T., Bartelmehs, K.L., Gibbs, G.V., & Boisen, M.B., Jr. (1993) Interactive software for calculating and displaying X-ray or neutron powder diffractometer patterns of crystalline materials. *American Mineralogist* **78**, 1104–1107.

Forman, S.A. & Peacock, M.A. (1949) Crystal Structure of rickardite $Cu_{4-x}Te_2$. *American Mineralogist* **34**, 441–451.

Ibers, J.A. & Hamilton, W.C., Eds. (1974) *International Tables for X-ray Crystallography, Volume IV*. Kynoch Press, Dordrecht, Netherlands.

Oxford Diffraction (2006) *CrysAlis* RED (Version 1.171.31.2) and ABSPACK in *CrysAlis* RED. Oxford Diffraction Ltd., Abingdon, Oxfordshire, England.

Pashinkin, A.S. & Fedorov, V.A. (2003) Phase equilibria in the Cu–Te system. *Inorganic Materials* **39**, 539–554.

Pertlik, F. (2001) Vulcanite, CuTe: hydrothermal synthesis and crystal structure refinement. *Mineralogy and Petrology* **71**, 149–154.

Roberts, A.C., Harris, D.C., Criddle, A.J., & Pinch, W.W. (1986) Cameronite, a new copper-silver telluride from the Good Hope mine, Vulcan, Colorado. *Canadian Mineralogist* **24**, 379–384.

Schutte, W.J. & de Boer, J.L. (1993) Determination of the incommensurately modulated structure of $Cu_{3-x}Te_2$. *Acta Crystallographica* **B49**, 398–403.

Sheldrick, G.M. (2008) A short history of SHELX. *Acta Crystallographica* **A64**, 112–122.

Suh, I.-K., Ohta, H., & Waseda, Y. (1988) High-temperature thermal expansion of six metallic elements measured by dilatation method and X-ray diffraction. *Journal of Materials Science* **23**, 757–760.

*Received June 3, 2014. Revised manuscript accepted July 10, 2014.*